Intelligent Automation & Soft Computing
DOI: 10.32604/iasc.2023.036601
Article

Tech Science Press

Backstepping Sliding Mode Control Based on Extended State Observer for Hydraulic Servo System

Zhenshuai Wan*, Yu Fu, Chong Liu and Longwang Yue

School of Mechanical and Electrical Engineering, Henan University of Technology, Zhengzhou, China
*Corresponding Author: Zhenshuai Wan. Email: wanzhenshuai@haut.edu.cn
Received: 06 October 2022; Accepted: 06 December 2022

Abstract: Hydraulic servo system plays an important role in industrial fields due to the advantages of high response, small size-to-power ratio and large driving force. However, inherent nonlinear behaviors and modeling uncertainties are the main obstacles for hydraulic servo system to achieve high tracking performance. To deal with these difficulties, this paper presents a backstepping sliding mode controller to improve the dynamic tracking performance and anti-interference ability. For this purpose, the nonlinear dynamic model is firstly established, where the nonlinear behaviors and modeling uncertainties are lumped as one term. Then, the extended state observer is introduced to estimate the lumped disturbance. The system stability is proved by using the Lyapunov stability theorem. Finally, comparative simulation and experimental are conducted on a hydraulic servo system platform to verify the efficiency of the proposed control scheme.

Keywords: Hydraulic servo system; nonlinear behaviors; modeling uncertainties; backstepping control; sliding mode control; extended state observer

1 Introduction

Hydraulic servo system has become increasingly popular in modern industrial automation and has been used in many fields [1–3], including aircraft actuators [4], rolling mills [5] and load simulators [6]. Compared to their electrical or pneumatic counterparts, hydraulic system demonstrates excellent superiorities of high precision, fast response, large power density, and compact structure [7–9]. However, precision motion control of hydraulic servo system is very hard due to inherent nonlinearities, time-variant loads, parametric uncertainties and uncertain disturbances [10–12]. In view of these drawbacks, how to achieve high precision control of hydraulic servo system has attracted great attentions in both academia and industries over the last decade. Although the traditional constant-gain controllers based on linear model are relatively mature, their global stability and tracking accuracy can hardly meet the real-time control requirements of modern industries [13]. Therefore, it is indispensable to build a dynamic mathematical model and design an advanced controller to improve the tracking performance and anti-interference ability of hydraulic servo system.

To obtain satisfactory control performance, many control methods have been developed, such as PID control [14], adaptive control [15], robust control [16], sliding mode control [17], fuzzy logic control [18]

and backstepping control [19]. The classical PID control is widely used in hydraulic servo system for its simple structure, clear function and easy realization. Nevertheless, strong nonlinearity and parameter uncertainty reduce the control performance when the operating point of the system changes [20]. Concerning that PID controller fails to solve the parameter variation and external disturbance, adaptive control is proposed to cope with variable working conditions due to its excellent online learning ability [21]. However, it is difficult for adaptive control to guarantee the system stability because the uncertain parameters of hydraulic servo system need to be linearized before they are processed [22]. That is to say, the nonlinear system is first transformed into the equivalent linear system by canceling out the nonlinear terms using feedback method [23]. Then, the mature linear control methods can be used in the nonlinear system. To further solve nonlinearities and uncertainties that cannot be presented in a linear parameter form, function approximation and fuzzy rules are adopted to approximate the matched and mismatched uncertainties [24–26]. However, the heavy computation burden and complicated convergence analysis restrict the practical application of adaptive control [27]. In order to effectively reduce the chattering of sliding mode control, the discontinuous sign function can be replaced by continuous functions, such as saturation functions, hyperbolic functions and switching functions [28–30]. The robust controller can guarantee a prescribed transient tracking performance and final tracking accuracy in existence of both modeled and unmodeled dynamics. However, the robust term adopting fixed boundaries rather than specific dynamic boundaries to roughly compensate for unmodeled dynamics makes the robust controller too conservative [31].

Compared to other control methods, backstepping control has attracted great interests due to its robustness to external disturbances and low sensitivity to parameter variations. As backstepping control implies, the high-order nonlinear system is decomposed into multiple first-order systems. The variables at the next step are taken as virtual input and acted on the current subsystem, and the Lyapunov function is established according to the system at the upper step to achieve system stability. Until the last step, the true control expression and the actual update law are obtained. To avoid the differential explosion of traditional backstepping method, Guo et al. used dynamic surface control to ease the computation burden and system singularity [32]. There are many researches on nonlinear control systems with various state observers, but they have limitations on disturbances, such as assumption uncertainties bounded and accurate expressions of disturbances [33]. Yang et al. proposed a neuroadaptive learning control scheme for electro-hydraulic servo constrained nonlinear system with disturbance, where the neural network was used to estimate the uncertainties and disturbances on-line and meanwhile compensate for them by using adaptive law [34]. In this paper, the disturbance of the hydraulic servo system is estimated by extending state observer and compensating them in a feedforward way by the backstepping method. The main contributions can be described as follows: (1) it has fewer design parameters and convenient parameters adjustment process. (2) it reduces the computational load and achieves excellent tracking performance in the case of various disturbances. (3) Owing to the designed extended state observer, the unmodeled disturbances are compensated actively. (4) The proposed controller is continuous and chattering-free, which is beneficial to practical applications.

The rest of this paper is organized as follows. Section 2 depicts the hydraulic servo system and presents the dynamical mathematical model. Section 3 provides the design of backstepping sliding mode controller based on extended state observer. Meanwhile, the stability analysis and convergence proof of the proposed controller are given respectively. Simulation and experiment results for the desired trajectory tracking control are given in Sections 4 and 5, respectively. Finally, some conclusions are drawn in Section 6.

2 Dynamical Mathematical Model of Hydraulic Servo System

The hydraulic servo systems are mainly composed of the electrical part, the hydraulic part and the mechanical part. The coupling between these parts deteriorates the nonlinear behaviors and modeling

uncertainties [35]. The schematic diagram of the hydraulic servo system studied in this paper is shown in Fig. 1. The pump delivers hydraulic fluid oil from the oil tank to hydraulic cylinder by servo valve. The accumulator acts as an auxiliary source of energy when additional power is suddenly required. The relief valve limits the maximum operating pressure and automatically regulates that the pressure does not exceed the specified value. The actuator drives the load to generate the desired torque/force outputs. The servo valve controls the direction of the actuator by adjusting the position of its spool.

Due to the fact that the dynamics of servo valve are much faster than the rest parts of system such that the dynamics can be neglected without loss of significance control performance. Thus, the dynamic equation of servo valve can be simplified as [36]

$$x_v = k_{sv}u \tag{1}$$

where x_v is the displacement of servo valve, k_{sv} is the gain constant of servo valve, u is the control signal.

The flow rate of servo valve is controlled by the valve orifice. Regardless of the leakage, the load flow equation of servo valve is given as

$$Q_L = C_d w x_v \sqrt{\frac{P_s - \text{sign}(u)P_L}{\rho}} \tag{2}$$

where $Q_L = (Q_1 + Q_2)$ is the real-time flow rates, where Q_1 is the supply flow and Q_2 is the return flow; C_d is the flow discharge coefficient; w is the area gradient of servo valve spool; ρ is the fluid oil mass density; P_s is the supply pressure; $P_L = P_1 - P_2$ is the differential pressure of actuator, where P_1 and P_2 are the pressures in each side of the cylinder. The sign function represents the change in the direction of flow fluid through the servo valve, which is the main nonlinear factors.

According to the flow conservation law, the flow-pressure equation of hydraulic cylinder is described as follows

$$Q_L = A\dot{y} + C_t P_L + \frac{V_t}{4\beta_e}\dot{P}_L \tag{3}$$

where A is the pressure area of the piston; y is the displacement of the cylindrical piston; C_t is the total leakage coefficient of the hydraulic actuator; V_t is the total volume of the actuator; β_e is the effective bulk modulus of the hydraulic fluid.

The piston of hydraulic servo system can be modeled as the classical mass-spring-viscous system. According to Newton's second law, the force balance equation of hydraulic actuator can be described by

$$AP_L = m\ddot{y} + B\dot{y} + Ky \tag{4}$$

where m is the mass of inertia load; K is the stiffness constant of spring; B is the damping coefficient of damper.

Define the system state variables $x = [x_1, x_2, x_3]^T = [y, \dot{y}, AP_L/m]^T$, then the state space representation of the hydraulic servo system can be formulated as

$$\begin{aligned}
\dot{x}_1 &= x_2 \\
\dot{x}_2 &= x_3 - \frac{B}{m}x_2 - \frac{K}{m}x_1 \\
\dot{x}_3 &= \frac{4\beta_e A C_d w k_{sv}}{mV_t}\sqrt{\frac{P_s - \text{sign}(u)(mx_3/A)}{\rho}}u - \frac{4\beta_e A^2}{mV_t}x_2 - \frac{4\beta_e C_t}{V_t}x_3
\end{aligned} \tag{5}$$

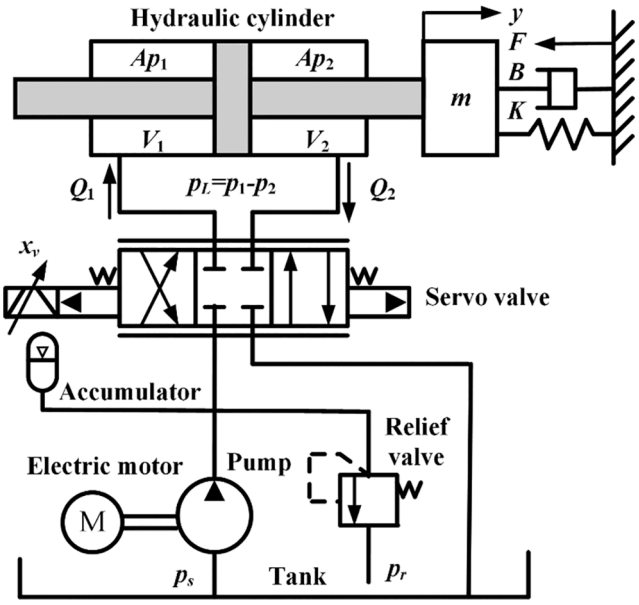

Figure 1: Schematic diagram of hydraulic servo system

For hydraulic servo systems, the parameters C_d, ρ, K, B, β_e and C_t are unknown positive constants. Considering nonlinear behaviors and modeling uncertainties, the state space model Eq. (5) can be rewritten as

$$\begin{aligned}\dot{x}_1 &= x_2\\ \dot{x}_2 &= x_3 + \bar{f}_2(x_1,x_2) + d_2(x_1,x_2)\\ \dot{x}_3 &= \bar{g}_3(x_3,u)u + \bar{f}_3(x_2,x_3) + d_3(x_1,x_2,x_3)\end{aligned} \tag{6}$$

where $\bar{f}_2(x_1,x_2) = -(\bar{B}/m)x_2 - (\bar{K}/m)x_1$; $\bar{f}_3(x_2,x_3) = -(4\bar{\beta}_e A^2/(mV_t))x_2 - (4\bar{\beta}_e\bar{C}_t/V_t)x_3$; $\bar{g}_3(x_3,u) = (4\bar{\beta}_e A\bar{C}_d w k_{sv}/(mV_t\sqrt{\bar{\rho}}))\sqrt{P_s - \text{sign}(u)(mx_3/A)}$, $\bar{B},\bar{K},\bar{\beta}_e,\bar{C}_d,\bar{\rho},\bar{C}_t$ are nominal values of uncertain parameters respectively; $d_2(x_1,x_2)$ and $d_3(x_1,x_2,x_3)$ are the lumped uncertain hydraulic parameters and unknown external loads respectively. d_2 and d_3 are bounded by $|d_2| \le d_{2\max}$ and $|d_3| \le d_{3\max}$.

3 Controller Design

The control objective is to design a controller to let the x_1 track the desired trajectory y_d as closely as possible in the presence of nonlinear behaviors and modeling uncertainties.

3.1 Extend State Observer Design

Extend d_2 as an additional state variable by defining $x_{e1} = d_2$, and d_3 as an additional state variable by defining $x_{e2} = d_3$, then the state variable is extended to $x = [x_1, x_2, x_{e1}, x_3, x_{e2}]$. Define $h_1(t)$ and $h_2(t)$ as the time derivative of x_{e1} and x_{e2} respectively. Then the system state representation can be rearranged as

$$\begin{aligned}\dot{x}_1 &= x_2\\ \dot{x}_2 &= x_3 + \bar{f}_2(x_1,x_2) + x_{e1}\\ \dot{x}_{e1} &= h_1(t)\\ \dot{x}_3 &= \bar{g}_3(x_3,u)u + \bar{f}_3(x_2,x_3) + x_{e2}\\ \dot{x}_{e2} &= h_2(t)\end{aligned} \tag{7}$$

The goal of the observer design is to estimate the lumped disturbances x_{e1} and x_{e2} for controller compensation in real time. Define $\hat{x}$ as the estimation of x and $\tilde{x} = x - \hat{x}$ as the estimation error. From the extended system model Eq. (7), the extended state observers are constructed as

$$\begin{aligned}
\dot{\hat{x}}_1 &= \hat{x}_2 + 3\omega_1(x_1 - \hat{x}_1) \\
\dot{\hat{x}}_2 &= \hat{x}_3 + \bar{f}_2(x_1, x_2) + 3\omega_1^2(x_1 - \hat{x}_1) \\
\dot{\hat{x}}_{e1} &= \omega_1^3(x_1 - \hat{x}_1) \\
\dot{\hat{x}}_3 &= \bar{g}_3(\hat{x}_3, u)u + \bar{f}_3(x_2, x_3) + 2\omega_2(x_1 - \hat{x}_1) \\
\dot{\hat{x}}_{e2} &= \omega_2^2(x_1 - \hat{x}_1)
\end{aligned} \tag{8}$$

where $\omega_1 > 0$ and $\omega_2 > 0$ are tunning parameters of the observer, which can be viewed as the bandwidths of the observer.

Combined with Eqs. (7) and (8), the dynamics of the state estimation errors can be written as

$$\begin{aligned}
\dot{\tilde{x}}_1 &= \tilde{x}_2 - 3\omega_1(x_1 - \hat{x}_1) \\
\dot{\tilde{x}}_2 &= \tilde{x}_3 + \tilde{f}_2(x_1, x_2) - 3\omega_1^2(x_1 - \hat{x}_1) \\
\dot{\tilde{x}}_{e1} &= h_1(t) - \omega_1^3(x_1 - \hat{x}_1) \\
\dot{\tilde{x}}_3 &= \tilde{g}_3(\tilde{x}_3, u)u + \tilde{f}_3(x_2, x_3) - 2\omega_2(x_3 - \hat{x}_3) \\
\dot{\tilde{x}}_{e2} &= h_2(t) - \omega_2^2(x_3 - \hat{x}_3)
\end{aligned} \tag{9}$$

where $\tilde{f}_2(x_1, x_2) = f_2(x_1, x_2) - f_2(\hat{x}_1, \hat{x}_2)$, $\tilde{g}_3(\tilde{x}_3, u) = g_3(x_3, u) - g_3(\hat{x}_3, u)$, $\tilde{f}_3(x_2, x_3) = f_3(x_2, x_3) - f_3(\hat{x}_2, \hat{x}_3)$.

Define $\gamma = [\gamma_1, \gamma_2, \gamma_3] = [\tilde{x}_1, \tilde{x}_2/\omega_{o1}, \tilde{x}_{e1}/\omega_{o1}^2]$, $\eta = [\eta_1, \eta_2] = [\tilde{x}_3, \tilde{x}_{e2}/\omega_{o2}]$, then Eq. (9) can be represented as

$$\begin{aligned}
\dot{\gamma} &= \omega_{o1} A_1 \gamma + B_1 \frac{h_1(t)}{\omega_{o1}^2} \\
\dot{\eta} &= \omega_{o2} A_2 \gamma + B_2 \frac{h_2(t)}{\omega_{o2}^2}
\end{aligned} \tag{10}$$

where

$$A_1 = \begin{bmatrix} -3 & 1 & 0 \\ -3 & 0 & 1 \\ -1 & 0 & 0 \end{bmatrix}, B_1 = \begin{bmatrix} 0 \\ 0 \\ 1 \end{bmatrix}, A_2 = \begin{bmatrix} -2 & 1 \\ -1 & 0 \end{bmatrix}, B_2 = \begin{bmatrix} 0 \\ 1 \end{bmatrix} \tag{11}$$

Note that A_1 and A_2 are Hurwitz, so there exists positive definite matrixes P_{11} and P_{12} satisfying the following equations

$$A_1{}^T P_{11} + P_{11} A_1{}^T = -I, A_2{}^T P_{22} + P_{22} A_2{}^T = -I \tag{12}$$

Define a positive definite function V_o as

$$V_o = \frac{1}{2}\gamma^T P_{11}\gamma + \frac{1}{2}\eta^T P_{22}\eta \tag{13}$$

The time derivative of V_o can be obtained as

$$\begin{aligned}\dot{V}_o &= \frac{1}{2}\left[\dot{\gamma}^T P_{11}\gamma + \gamma^T P_{11}\dot{\gamma}\right] + \frac{1}{2}\left[\eta^T P_{22}\eta + \eta^T P_{22}\eta\right] \\ &= -\frac{1}{2}\omega_{o1}\|\gamma\|^2 + \gamma^T P_{11}B_1\frac{h_1(t)}{\omega_{o1}^2} - \frac{1}{2}\omega_{o2}\|\eta\|^2 + \eta^T P_{22}B_2\frac{h_2(t)}{\omega_{o2}}\end{aligned} \tag{14}$$

The upper bound of Eq. (14) can be achieved by

$$\dot{V}_o \le -\frac{1}{2}\left(\omega_{o1} - \frac{\|P_{11}B_1\|}{\omega_{o1}^4}\right)\|\gamma\|^2 - \frac{1}{2}\left(\omega_{o2} - \frac{\|P_{22}B_2\|}{\omega_{o2}^2}\right)\|\eta\|^2 + \frac{|h_1|_{\max}^2 + |h_2|_{\max}^2}{2} \tag{15}$$

Define $h_0 = (|h_1|_{\max}^2 + |h_2|_{\max}^2)/2$, $\kappa = \min\left\{\omega_{o1} - \|P_{11}B_1\|/\omega_{o1}^4, \omega_{o2} - \|P_{22}B_2\|/\omega_{o2}^2\right\}$, then the Eq. (15) can be rewritten as

$$\dot{V}_o \le -\lambda V_0 + h_0 \tag{16}$$

where $\lambda = 0.5\lambda\min\{1, 1/\lambda_{\max}(P_{11}), 1/\lambda_{\max}(P_{22})\}$.

Integrating Eq. (16), $\dot{V}_o$ yields

$$V_o \le \exp(-\lambda t)V_0 + \frac{h_0}{\lambda}[1 - \exp(-\lambda t)] \tag{17}$$

According to Eq. (17), it can be indicated that state estimation and tracking error estimation are guaranteed to be bounded. Moreover, the extended state error can be regulated arbitrarily small by increasing the bandwidth tunning parameters.

3.2 Controller Design

Define sliding surface for each state variable

$$s_i = x_i - \alpha_{i-1} \tag{18}$$

where i = 1,2,3, α_{i-1} is the estimation of x_i, and s_i can converge to zero by the proper selection of α_{i-1}. In particular, $\alpha_0 = y_d$.

The sliding mode surface for the first subsystem is defined as $s_1 = x_1 - y_d$, then

$$\dot{s}_1 = \dot{x}_1 - \dot{y}_d = x_2 - \dot{y}_d = s_2 + \alpha_1 - \dot{y}_d \tag{19}$$

Choose the virtual control item α_1 as $\alpha_1 = -k_1 s_1 + \dot{y}_d$. The Lyapunov function for the first subsystem is designed as

$$V_1 = \frac{1}{2}s_1^2 \tag{20}$$

where k_1 is positive definite. Then the derivative of V_1 can be derived as

$$\dot{V}_1 = s_1\dot{s}_1 = s_1(s_2 + \alpha_1 - \dot{y}_d) = s_1(s_2 - k_1 s_1 + \dot{y}_d - \dot{y}_d) = -k_1 s_1^2 + s_1 s_2 \tag{21}$$

The sliding mode surface for the second subsystem is defined as $s_2 = x_2 - \alpha_1$, then the time derivative of s_2 can be written as

$$\begin{aligned}\dot{s}_2 &= \dot{x}_2 - \dot{\alpha}_1 = x_3 + \bar{f}_2(x_1, x_2) + d_2(x_1, x_2) - \frac{\partial \alpha_1}{\partial x_1}\dot{x}_1 - \frac{\partial \alpha_1}{\partial y_d} {y_d}^{(2)} \\ &= s_3 + \alpha_2 + \bar{f}_2(x_1, x_2) - \frac{\partial \alpha_1}{\partial x_1} x_2 - \frac{\partial \alpha_1}{\partial y_d} {y_d}^{(2)} + d_2(x_1, x_2)\end{aligned} \tag{22}$$

In order to make the second subsystem to reach the sliding mode surface, the virtual control item is defined as

$$\alpha_2 = -k_2 s_2 - s_1 - \bar{f}_2(x_1, x_2) + \frac{\partial \alpha_1}{\partial x_1}\dot{x}_1 + \frac{\partial \alpha_1}{\partial y_d} {y_d}^{(2)} - d_2(x_1, x_2)\frac{\mu_2 s_2}{\sqrt{s_2^2 + \varepsilon_2^2}} \tag{23}$$

where k_2 is positive definite, $\mu_2 > 1$ and $0 < \epsilon_2 < 1$ are positive performance constants.

The Lyapunov function for the second subsystem is given by

$$V_2 = V_1 + \frac{1}{2} s_2^2 \tag{24}$$

Thus, the time derivative of V_2 can be derived as

$$\dot{V}_2 = \dot{V}_1 + s_2 \dot{s}_2 \le -k_1 s_1^2 + s_1 s_2 + s_2 \dot{s}_2 \tag{25}$$

Substituting Eqs. (22) and (23) into Eq. (25)

$$\begin{aligned}\dot{V}_2 &\le -k_1 s_1^2 - k_2 s_2^2 + s_2 s_3 - d_2(x_1, x_2)\frac{\mu_2 s_2^2}{\sqrt{s_2^2 + \epsilon_2^2}} + s_2 d_2(x_1, x_2) \\ &\le -k_1 s_1^2 - k_2 s_2^2 + s_2 s_3 - |s_2| d_2(x_1, x_2)\frac{\mu_2 |s_2|}{\sqrt{s_2^2 + \epsilon_2^2}} + |s_2| d_2(x_1, x_2) \\ &= -k_1 s_1^2 - k_2 s_2^2 + s_2 s_3 - |s_2| d_2(x_1, x_2)\left(\frac{\mu_2 |s_2|}{\sqrt{s_2^2 + \epsilon_2^2}} - 1\right)\end{aligned} \tag{26}$$

To ensure the stability of the second subsystem, $|s_2| > \epsilon_2 / \sqrt{\mu_2^2 - 1}$. Then the Eq. (24) can be rewritten as

$$\dot{V}_2 = \dot{V}_1 + s_2 \dot{s}_2 \le -k_1 s_1^2 - k_2 s_2^2 + s_2 s_3 \tag{27}$$

Similarly, the sliding mode surface for the third subsystem is defined as $s_3 = x_3 - \alpha_2$, then the time derivative of s_3 can be written as

$$\begin{aligned}\dot{s}_3 &= \dot{x}_3 - \dot{\alpha}_2 \\ &= \bar{g}_3(x_3, u) + \bar{f}_3(x_1, x_2, x_3) + d_3(x_1, x_2 . x_3) - \sum_{j=1}^{2} \frac{\partial \alpha_2}{\partial x_j}\dot{x}_j - \sum_{k=1}^{2} \frac{\partial \alpha_2}{\partial {y_d}^{(k)}} {y_d}^{(k+1)} \\ &= \bar{g}_3(x_3, u) + \bar{f}_3(x_1, x_2, x_3) - \frac{\partial \alpha_2}{\partial x_1} x_2 - \frac{\partial \alpha_2}{\partial x_2}\left(x_3 + \bar{f}_2(x_1, x_2)\right) \\ &- \frac{\partial \alpha_2}{\partial y_d} {y_d}^{(2)} - \frac{\partial \alpha_2}{\partial {y_d}^{(2)}} {y_d}^{(3)} - \frac{\partial \alpha_2}{\partial x_2} d_2(x_1, x_2) + d_3(x_1, x_2 . x_3)\end{aligned} \tag{28}$$

Now, choosing the real control signal as

$$\begin{aligned} u_b = & \frac{1}{\bar{g}_3(x_3,u)}\left(-k_3 s_3 - s_2 - \bar{f}_3(x_1,x_2,x_3) + \frac{\partial \alpha_2}{\partial x_1}x_2 + \frac{\partial \alpha_2}{\partial x_2}(x_3 + \bar{f}_2(x_1,x_2))\right) \\ & + \frac{1}{\bar{g}_3(x_3,u)}\left(\frac{\partial \alpha_2}{\partial y_d}{y_d}^{(2)} + \frac{\partial \alpha_2}{\partial {y_d}^{(2)}}{y_d}^{(3)} - \left(d_3(x_1,x_2,x_3) - \frac{\partial \alpha_2}{\partial x_2}d_2(x_1,x_2)\right)\mathrm{sgn}(s_3)\right) \end{aligned} \tag{29}$$

where k_3 is positive definite. The candidate Lyapunov function for the third subsystem is given by

$$V_3 = V_2 + \frac{1}{2}s_3^2 \tag{30}$$

The first-order differential of the candidate Lyapunov function is given as

$$\begin{aligned} \dot{V}_3 &= \dot{V}_2 + s_3\dot{s}_3 \\ &\le -k_1 s_1^2 - k_2 s_2^2 + s_3 s_2 + s_3(-k_3 s_3 - s_2 - d_{\Delta 3}\mathrm{sgn}(s_3) + \tilde{d}_{\Delta 3}) \\ &\le -k_1 s_1^2 - k_2 s_2^2 - k_3 s_3 - |s_3|\bar{d}_{\Delta 3} + s_3\tilde{d}_{\Delta 3} \\ &\le -k_1 s_1^2 - k_2 s_2^2 - k_3 s_3^2 \end{aligned} \tag{31}$$

where $d_{\Delta 3} = \sum_{j=1}^{2}\frac{\partial \alpha_2}{\partial x_j}d_j(\bar{x}_j) + d_3(\bar{x}_3)$, $|d_{\Delta 3}| \le \bar{d}_{\Delta 3}$, $\bar{d}_{\Delta 3}$ is a positive constant, $\tilde{d}_{\Delta 3} = \bar{d}_{\Delta 3} - \hat{d}_{\Delta 3}$.

According to Lyapunov theory, the dynamic system is globally asymptotically stable, which implies that the error will converge to zero even in the face of nonlinear behaviors and modeling uncertainties.

4 Simulation Results

The comparative simulations are conducted in MATLAB/Simulink software. The parameters of hydraulic system are selected as: m = 300 kg, $V_t = 9 \times 10^{-5}\mathrm{m}^3$, ρ = 900 kg/m^3, $A = 3.14 \times 10^{-4}\mathrm{m}^2$, K = 1500 N/m, B = 1200 N·s/m, $C_t = 4 \times 10^{-3}$, $k_{sv} = 5.9 \times 10^{-7}$ m/V, C_d = 0.62, $\beta_e = 6.9 \times 10^8$ Pa. In order to verify the effectiveness of the proposed controller, PID and backstepping controllers are tested for comparison. (1) PID: the control gains are set as K_p = 200, K_i = 80, K_d = 0.01, which is adjusted by a heuristic tunning method for small steady-state error and good transient response. (2) Backstepping: the constants are set as $k_1 = k_2 = k_3 = 2$, $\mu_2 = 1.5$, $\varepsilon_2 = 0.6$. (3) Presented controller: the bandwidths are set as ω_{o1} = 400, ω_{o2} = 600, the constants are set as $k_1 = k_2 = k_3 = 5$, $\mu_2 = 1.5$, $\varepsilon_2 = 0.6$. In particular, the parameters of these three controllers are well tuned with many times trial-and-error procedure to obtain satisfactory performance.

To simulate the nonlinear characteristics and external disturbances, the measurement noise of the displacement sensor and the input noise are 0.2% and 0.5% of the maximum ranges, respectively. The comparative tracking performance for sine motion with amplitude 10 mm and frequency 1 Hz is shown in Fig. 2. It can be seen that the presented controller can eliminate or attenuate the influence of lumped uncertainties better than the PID controller and backstepping controller. The tracking errors of different controllers are shown in Fig. 3. It is noted that the tracking errors of PID and backstepping have large chattering due to the lumped uncertainties and measurement noise. However, the presented controller achieves better disturbance compensation and smaller tracking error than the other two controllers. Specifically, the maximum trajectory error for PID and backstepping is 1.1 and 0.8 mm, respectively. The tracking error of presented controller is relatively very small, mostly within the 0.4 mm, which verifies the effectiveness of the presented control strategy.

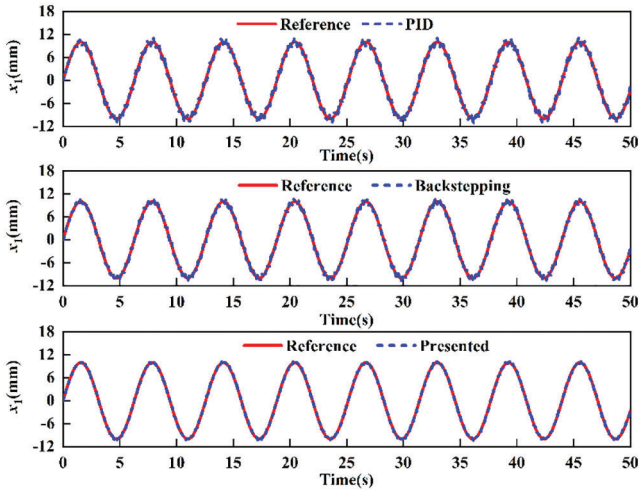

Figure 2: Comparative tracking performance for sine motion

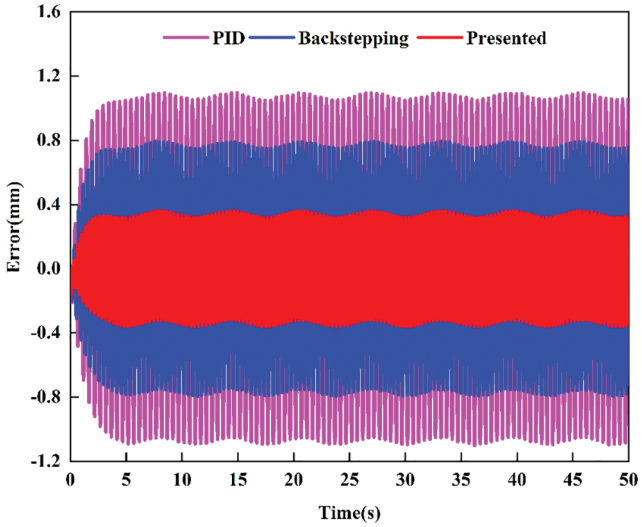

Figure 3: Comparative tracking errors for sine motion

Both the estimations x_{e1} and x_{e2} are shown in Fig. 4. The estimated states track the actual states quite well, which means that the observer has better tracking performance for the extend state although the system is subjected to external disturbance. Fig. 5 shows control input of three controllers. The proposed controller is free of chattering, which implies that it can successfully tackle the chattering problem and is easy to implement.

To quantitatively evaluate the tracking performance of different controllers, three error indices mean value of the absolute error, standard deviation of absolute error and integral of time multiplied by absolute error are defined as follows

$$\begin{cases} \mu = \dfrac{1}{N}\displaystyle\sum_{i=1}^{N} |e_1(i)| \\ \sigma = \sqrt{\dfrac{1}{N}\displaystyle\sum_{i=1}^{N} (|e_1(i)| - \mu)^2} \\ E = \dfrac{1}{N}\displaystyle\sum_{i=1}^{N} iT_s|e_1(i)| \end{cases} \tag{32}$$

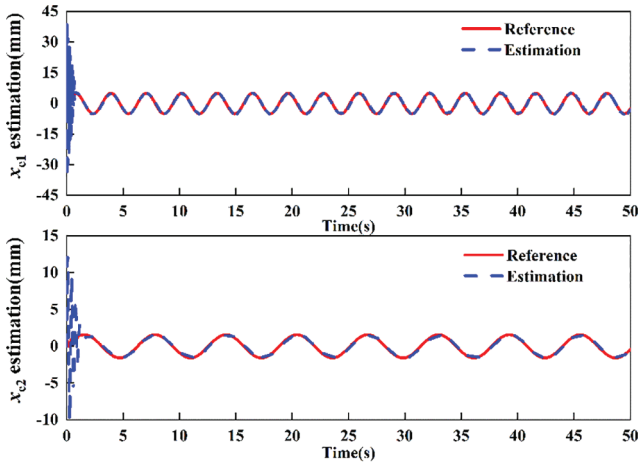

Figure 4: External disturbance estimation of presented controller

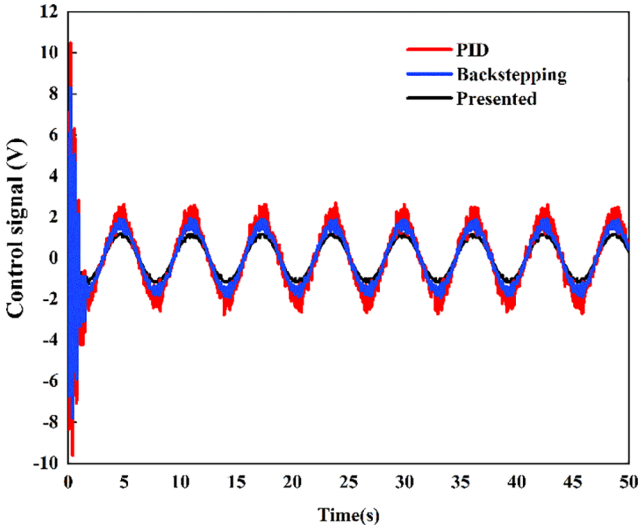

Figure 5: Control signal of presented controller

The performance indices of the different controllers are given in Table 1. For PID controller, the absolute error is about 0.6879 mm. For backstepping controller, the absolute error is reduced to 0.488 mm. For the presented controller, the absolute error is reduced to only 0.2156 mm. It can be seen that the proposed controller outperforms the other two controllers in terms of the other two performance indices, which

means that the proposed control scheme is very helpful to alleviate the effects of nonlinear characteristics and external disturbance in hydraulic servo system.

Table 1: Comparation performance indices

Indices	μ	σ	E
PID	0.6879	0.3295	0.6847
Backstepping	0.4888	0.2373	0.3952
Presented	0.2156	0.1056	0.1767

5 Experiment Results

Fig. 6 shows the control scheme block diagram of hydraulic servo system. The host PC can monitor and send the command signal to the signal conditioner, where the control program is built by Matlab/Simulink. The DAC interface transforms digital signal into analogue signal. The power amplifier is used to enlarge the control signal and then drive the hydraulic actuator. The measured displacement and pressure signals acquired by sensors are sent to signal conditioner. The control objective of hydraulic servo system is to keep the actuator reproduce the desired signal as closely as possible. It should be noted that the parameters of the controller are consistent with those of simulation.

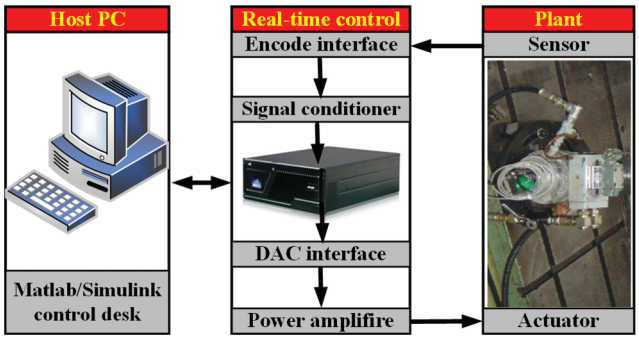

Figure 6: Control scheme block diagram of hydraulic servo system

The position comparative tracking performance for sine signal is given in Fig. 7 and their tracking errors are shown in Fig. 8. The experimental results show that the PID controller has maximum tracking error. The presented controller has a better tracking performance in terms of both disturbance compensation and error aspect than PID controller. Backstepping controller has an intermediate tracking error as compared to the presented controller and PID controller. Fig. 9 shows the control signal generated by controller, which is sent to servo valve of hydraulic system. When the PID controller is subjected to an external disturbance, a larger control signal is obviously produced. Whereas, the presented controller generates a low amplitude and fairly smooth control signal, which is critical to control system for energy minimization. The main reason why the proposed controller is more excellent compared with those controllers is that ESO is used to estimate lumped uncertainties and achieve active compensation.

The comparative tracking performance of the above controllers for square signal is shown in Fig. 10, and the tracking error curve is presented in Fig. 11. Obviously, the backstepping controller exhibits better performance than the PID controller. The maximum tracking error of backstepping is 0.6 mm; conversely, the PID controller has maximum error of 1 mm. However, the maximum position tracking error for the presented controller is only 0.4 mm.

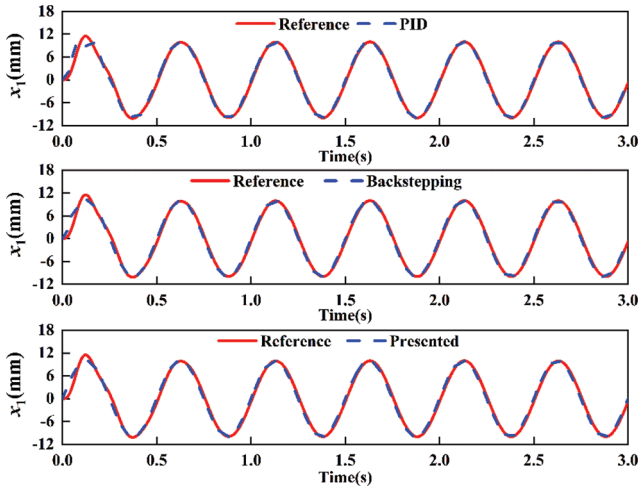

Figure 7: Comparative tracking performance for sine signal

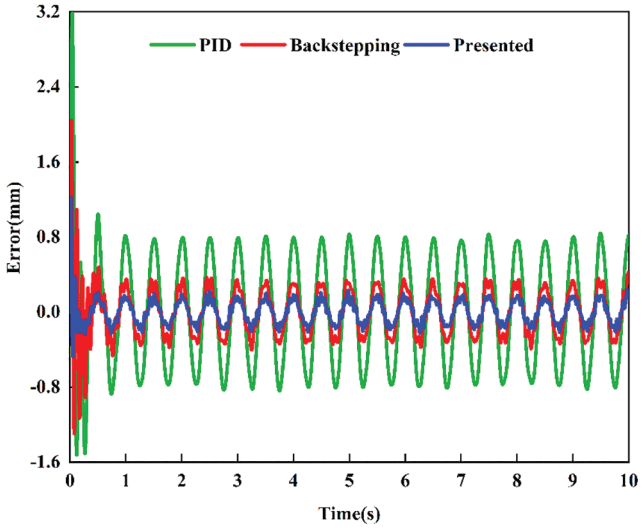

Figure 8: Comparative tracking error for sine signal

The comparisons of position tracking and position tracking error for multi-frequency sine signal are shown in Figs. 12 and 13. The standard deviation of absolute error of PID, backstepping and proposed controllers is 0.3123, 0.1738 and 0.1351 mm, respectively. The results indicate that the proposed controller can track the desired signal well, while PID controller and backstepping controller do not realize good tracking performance.

The concerned performance indices of different controllers for sine signal, square signal and multi-frequency sine signal are summarized in Fig. 14. For sine input signal, the μ of three controllers is about 0.5199, 0.2073 and 0.1047 mm. It is shown that the proposed controller outperforms the other two controllers again in terms of tracking precision. For square input signal, the σ of PID controller is about 0.2307 mm, the σ of backstepping controller is reduced to 0.1467 mm, the σ of presented controller is reduced to only 0.0826 mm. The smaller σ indicates the smoother tracking response, which is important for the steady-state performance of hydraulic servo system. For multi-frequency sine signal, the E of PID controller, backstepping controller and proposed controller is 0.3273, 0.1749 and 0.1438 mm,

respectively. It is also found that the proposed method has the smallest three tracking errors and highest control precision. For three typical input signals, the proposed controller has better tracking performance than the other two controllers.

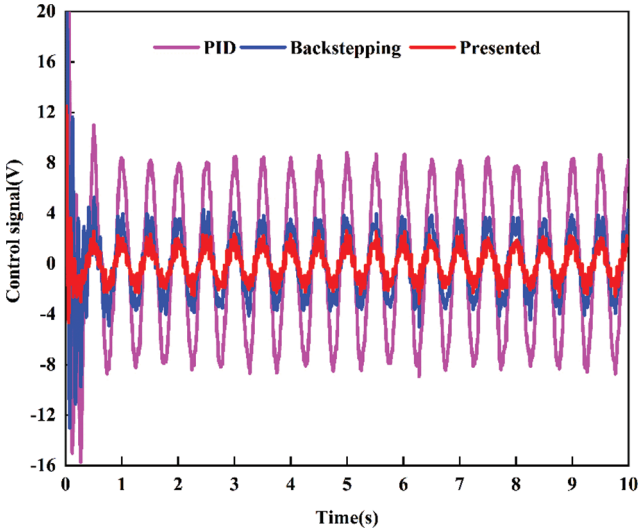

Figure 9: Comparative control signal for sine signal

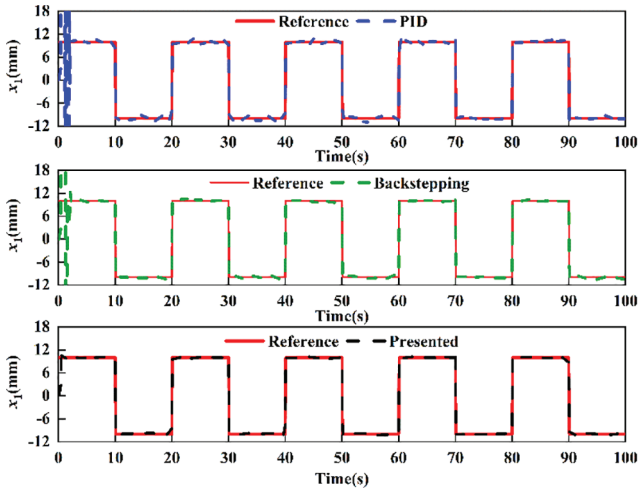

Figure 10: Comparative tracking performance for square signal

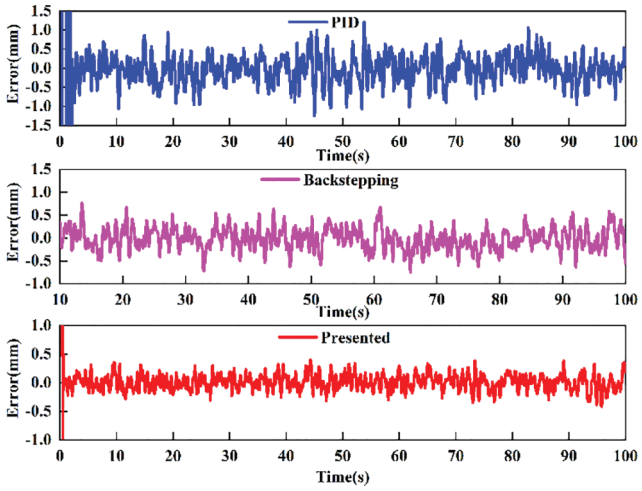

Figure 11: Comparative tracking error for square signal

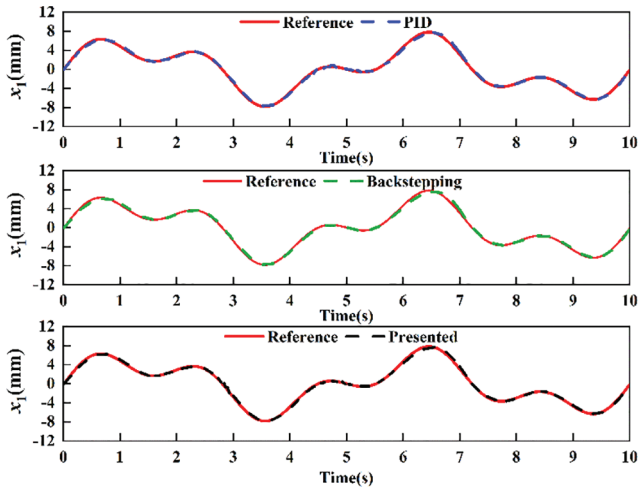

Figure 12: Comparative position tracking for multi-frequency sine signal

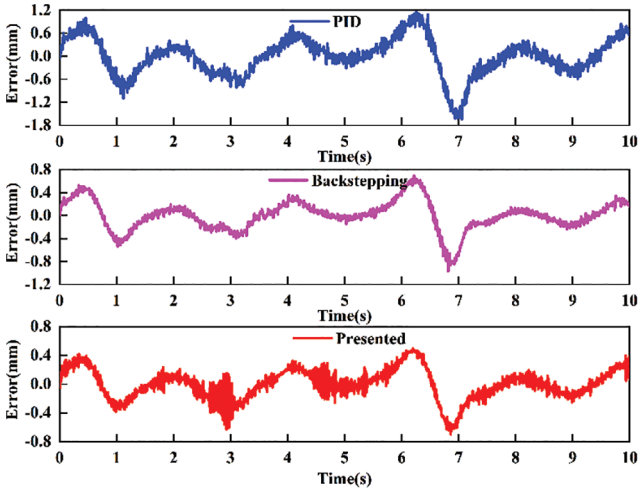

Figure 13: Comparative tracking error for multi-frequency sine signal

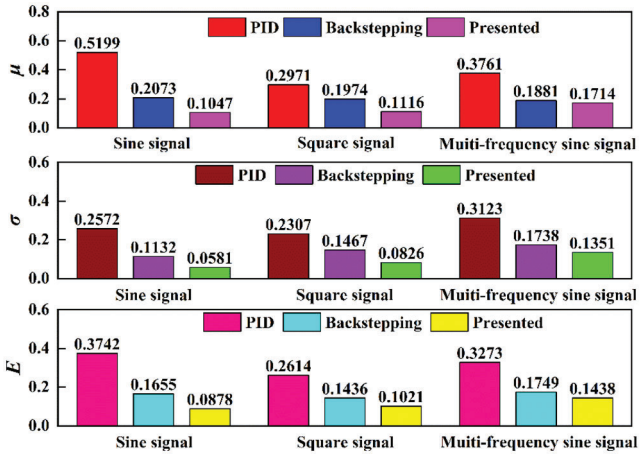

Figure 14: Comparation performance indices for different input signal

6 Conclusion

In this paper, a backstepping sliding mode control based on extended state observer is developed for the high precision tracking control of hydraulic servo system. The dynamic mathematical model of state space representation considering nonlinear characteristics and external disturbances is first constructed. Then, the extended state observation is introduced to estimate the lumped uncertainties. The controller is capable of forcing the position of the hydraulic servo system to track the desired trajectory in finite time and has robust behavior. The system stability is verified by Lyapunov criteria. Simulation and experimental comparative results validate the effectiveness of the proposed controller as compared to the PID controller and backstepping control.

Acknowledgement: The authors thank their families and colleagues for their continued support.

Funding Statement: The work is supported by the Key Science and Technology Program of Henan Province (Grant No. 222102220104), the Science and Technology Key Project Foundation of Henan Provincial Education Department (Grant No. 23A460014) and the High Level Talent Foundation of Henan University of Technology (Grant No. 2020BS043).

Conflicts of Interest: The authors declare that they have no conflicts of interest to report regarding the present study.

References

[1] K. Guo, M. Li, W. Shi and Y. Pan, "Adaptive tracking control of hydraulic systems with improved parameter convergence," *IEEE Transactions on Industrial Electronics*, vol. 69, no. 7, pp. 7140–7150, 2022.

[2] X. W. Yang, W. X. Deng, J. Y. Yao and X. L. Liang, "Asymptotic adaptive tracking control and application to mechatronic systems," *Journal of the Franklin Institute-Engineering and Applied Mathematics*, vol. 358, no. 12, pp. 6057–6073, 2021.

[3] Z. L. Chen, Q. Guo, H. Y. Xiong, D. Jiang and Y. Yan, "Control and implementation of 2-DOF lower limb exoskeleton experiment platform," *Chinese Journal of Mechanical Engineering*, vol. 34, no. 1, pp. 1–17, 2021.

[4] Z. B. Xu, G. L. Qi, Q. Y. Liu and J. Y. Yao, "ESO-based adaptive full state constraint control of uncertain systems and its application to hydraulic servo systems," *Mechanical Systems and Signal Processing*, vol. 167, no. 3, pp. 108560, 2022.

[5] Y. Tang, Z. C. Zhu, G. Shen, G. C. Rui, D. Cheng *et al.,* "Real-time nonlinear adaptive force tracking control strategy for electrohydraulic systems with suppression of external vibration disturbance," *Journal of the Brazilian Society of Mechanical Sciences and Engineering*, vol. 41, no. 7, pp. 278, 2019.

[6] J. S. Zhao, G. Shen, C. F. Yang, W. D. Zhu and J. Y. Yao, "A robust force feed-forward observer for an electro-hydraulic control loading system in flight simulators," *ISA Transactions*, vol. 89, no. 1, pp. 198–217, 2019.

[7] G. Palli, S. Strano and M. Terzo, "Sliding-mode observers for state and disturbance estimation in electro-hydraulic systems," *Control Engineering Practice*, vol. 74, no. 9, pp. 58–70, 2018.

[8] W. C. Sun, H. J. Gao and B. Yao, "Adaptive robust vibration control of full-car active suspensions with electrohydraulic actuators," *IEEE Transactions on Control Systems Technology*, vol. 21, no. 6, pp. 2417–2422, 2013.

[9] X. Li, Z. C. Zhu and G. Shen, "A switching-type controller for wire rope tension coordination of electro-hydraulic-controlled double-rope winding hoisting systems," *Proceedings of the Institution of Mechanical Engineers Part I-Journal of Systems and Control Engineering*, vol. 230, no. 10, pp. 1126–1144, 2016.

[10] M. Fallahi, M. Zareinejad, K. Baghestan, A. Tivay, S. M. Rezaei *et al.,* "Precise position control of an electro-hydraulic servo system via robust linear approximation," *ISA Transactions*, vol. 80, no. 11, pp. 503–512, 2018.

[11] D. Won, W. Kim and M. Tomizuka, "High-gain-observer-based integral sliding mode control for position tracking of electrohydraulic servo systems," *IEEE-ASME Transactions on Mechatronics*, vol. 22, no. 6, pp. 2695–2704, 2017.

[12] J. Park, B. Lee, S. Kang, P. Y. Kim and H. J. Kim, "Online learning control of hydraulic excavators based on echo-state networks," *IEEE Transactions on Automation Science and Engineering*, vol. 14, no. 1, pp. 249–259, 2017.

[13] M. E. M. Essa, M. A. S. Aboelela, M. A. M. Hassan and S. M. Abdrabbo, "Model predictive force control of hardware implementation for electro-hydraulic servo system," *Transactions of the Institute of Measurement and Control*, vol. 41, no. 5, pp. 1435–1446, 2019.

[14] G. Wrat, M. Bhola, P. Ranjan, S. K. Mishra and J. Das, "Energy saving and fuzzy-PID position control of electro-hydraulic system by leakage compensation through proportional flow control valve," *ISA Transactions*, vol. 101, no. 5, pp. 269–280, 2020.

[15] S. Chen, Z. Chen, B. Yao, X. C. Zhu, S. Q. Zhu *et al.,* "Adaptive robust cascade force control of 1-DOF hydraulic exoskeleton for human performance augmentation," *IEEE-ASME Transactions on Mechatronics*, vol. 22, no. 2, pp. 589–600, 2017.

[16] T. A. Davis, Y. C. Shin and B. Yao, "Adaptive robust control of machining force and contour error with tool deflection using global task coordinate frame," *Proceedings of the Institution of Mechanical Engineers Part B-Journal of Engineering Manufacture*, vol. 232, no. 1, pp. 40–50, 2018.

[17] C. Cheng, S. Y. Liu and H. Z. Wu, "Sliding mode observer-based fractional-order proportional-integral-derivative sliding mode control for electro-hydraulic servo systems," *Proceedings of the Institution of Mechanical Engineers Part C-Journal of Mechanical Engineering Science*, vol. 234, no. 10, pp. 1887–1898, 2020.

[18] W. M. Bessa, M. S. Dutra and E. Kreuzer, "Sliding mode control with adaptive fuzzy dead-zone compensation of an electro-hydraulic servo-system," *Journal of Intelligent and Robotic Systems*, vol. 58, no. 4, pp. 3–16, 2010.

[19] Q. Guo, Y. Zhang, B. G. Celler and S. W. Su, "Backstepping control of electro-hydraulic system based on extended-state-observer with plant dynamics largely unknown," *IEEE Transactions on Industrial Electronics*, vol. 63, no. 11, pp. 6909–6920, 2016.

[20] G. P. Liu and S. Daley, "Optimal-tuning PID controller design in the frequency domain with application to a rotary hydraulic system," *Control Engineering Practice*, vol. 8, no. 9, pp. 1045–1053, 2000.

[21] Z. Chen, F. H. Huang, C. N. Yang and B. Yao, "Adaptive fuzzy backstepping control for stable nonlinear bilateral teleoperation manipulators with enhanced transparency performance," *IEEE Transactions on Industrial Electronics*, vol. 67, no. 1, pp. 746–756, 2020.

[22] J. Jiang, J. Guo, B. Yao and Q. W. Chen, "Adaptive robust control of mobile satellite communication system with disturbance and model uncertainties," *Journal of Systems Engineering and Electronics*, vol. 23, no. 5, pp. 761–767, 2012.

[23] Z. B. Xu, D. W. Ma, J. Y. Yao and N. Ullah, "Feedback nonlinear robust control for hydraulic system with disturbance compensation," *Proceedings of the Institution of Mechanical Engineers Part I-Journal of Systems and Control Engineering*, vol. 230, no. 9, pp. 978–987, 2016.

[24] T. Gao, Y. J. Liu, L. Liu and D. Li, "Adaptive neural network-based control for a class of nonlinear pure-feedback systems with time-varying full state constraints," *IEEE-CAA Journal of Automatica Sinica*, vol. 5, no. 5, pp. 923–933, 2018.

[25] Y. J. Liu, Q. Zeng, L. Liu and S. C. Tong, "An adaptive neural network controller for active suspension systems with hydraulic actuator," *IEEE Transactions on Systems Man Cybernetics-Systems*, vol. 50, no. 12, pp. 5351–5360, 2020.

[26] Z. K. Yao, Y. P. Yu and J. Y. Yao, "Artificial neural network-based internal leakage fault detection for hydraulic actuators: An experimental investigation," *Proceedings of the Institution of Mechanical Engineers Part I-Journal of Systems and Control Engineering*, vol. 232, no. 4, pp. 369–382, 2018.

[27] Z. H. U. Dachang, "Sliding mode synchronous control for fixture clamps system driven by hydraulic servo systems," *Proceedings of the Institution of Mechanical Engineers Part C-Journal of Mechanical Engineering Science*, vol. 221, no. 9, pp. 1039–1045, 2007.

[28] K. Shao, J. C. Zheng, K. Huang, H. Wang, Z. H. Man *et al.,* "Finite-time control of a linear motor positioner using adaptive recursive terminal sliding mode," *IEEE Transactions on Industrial Electronics*, vol. 67, no. 8, pp. 6659–6668, 2020.

[29] J. Y. Yao, W. X. Deng and Z. X. Jiao, "RISE-based adaptive control of hydraulic systems with asymptotic tracking," *IEEE Transactions on Automation Science and Engineering*, vol. 14, no. 3, pp. 1524–1531, 2017.

[30] K. Shao, J. H. Zheng, H. Wang, X. Q. Wang and B. Liang, "Leakage-type adaptive state and disturbance observers for uncertain nonlinear sytems," *Nonlinear Dynamics*, vol. 105, no. 3, pp. 2299–2311, 2021.

[31] J. Y. Yao, Z. X. Jiao and B. Yao, "Robust control for static loading of electro-hydraulic load simulator with friction compensation," *Chinese Journal of Aeronautics*, vol. 25, no. 6, pp. 954–962, 2012.

[32] Q. Guo, Y. L. Liu, D. Jiang, Q. Wang, W. Y. Xiong *et al.,* "Prescribed performance constraint regulation of electrohydraulic control based on backstepping with dynamic surface," *Applied Sciences-Basel*, vol. 8, no. 1, pp. 76, 2018.

[33] M. J. Li, J. H. Wei, J. H. Fang, W. Z. Shi and K. Guo, "Fuzzy impedance control of an electro-hydraulic actuator with an extended disturbance observer," *Frontiers of Information Technology & Electronic Engineering*, vol. 20, no. 9, pp. 1221–1233, 2019.

[34] G. Yang, J. Y. Yao and Z. Dong, "Neuroadaptive learning algorithm for constrained nonlinear systems with disturbance rejection," *International Journal of Robust and Nonlinear Control*, vol. 32, no. 10, pp. 6127–6147, 2022.

[35] S. Wang, H. Yu, J. Yu, J. Na and X. Ren, "Neural-network-based adaptive funnel control for servo mechanisms with unknown dead-zone," *IEEE Transactions on Cybernetics*, vol. 50, no. 4, pp. 1383–1394, 2020.

[36] G. Shen, Z. C. Zhu, J. S. Zhao, W. D. Zhu, Y. Tang *et al.,* "Real-time tracking control of electro-hydraulic force servo systems using offline feedback control and adaptive control," *ISA Transactions*, vol. 67, no. 2, pp. 356–370, 2017.